

Invariance Guarantees using Continuously Parametrized Control Barrier Functions

Inkyu Jang¹ and H. Jin Kim^{1*}

¹Department of Aerospace Engineering, Seoul National University,
Seoul, 08826, Korea (janginkyu.larr@gmail.com, hjinkim@snu.ac.kr) * Corresponding author

Abstract: Control barrier function (CBF) is a famous tool used to guarantee set invariance. Inspired by the CBF framework, this paper introduces the notion of parametrized control barrier function (PCBF), a continuous spectrum of CBFs whose parameter space is a differentiable manifold. An optimization-based control strategy that uses PCBF and quadratic programming (QP), namely PCBF-QP, is proposed. PCBF-QP is capable of ensuring invariance of its level set, and it makes the best use of the differentiable structure of the parameter space to expand the feasible region of the optimization, allowing the system to select its control input from a broader range. The proposed control strategy is validated in two different simulation experiments. The results clearly show that in both scenarios, PCBF-QP successfully filters the reference to generate an input sequence that constrains the state trajectory in a prescribed bound.

Keywords: Control barrier function, safety-critical control

1. INTRODUCTION

Set invariance is a key concept in control theory that plays a crucial role in ensuring safety of a system [1–3]. Recently, control barrier function (CBF) [4] has emerged as a powerful tool for achieving set invariance by encoding the constraints in a single differentiable scalar function defined on the state space. Leveraging this property, one can build a real-time controller (or a safety filter in some perspective) based on quadratic programming (QP), namely CBF-QP [5]. Focusing on its simplicity and the ease of synthesizing a safety-critical controller, many variants of CBFs have been proposed, such as robust CBF [6], adaptive CBF [7], CBF for systems with high relative degree [8, 9], and CBF for multi-agent scenarios [10].

In this work, we show that a differentiable parametrized spectrum of CBFs, which we call parametrized CBF (PCBF), can be used to guarantee invariance of a set. A QP-based control strategy using PCBF, namely PCBF-QP, is proposed. PCBF-QP selects the input that minimally deviates from the given reference input while constraining the state and the parameter in a prescribed region. We find that, compared to the original CBF-QP, the proposed method provides a broader feasible region for the optimization-based controller. This is due to the differentiable structure of the parameter space: PCBF-QP is capable of selecting input that exceeds the CBF constraints by choosing nonzero parameter speed.

Many real-world applications involve CBFs that can be continuously parametrized. For instance, the value function that describes a backward reachable tube (BRT) [11] can be treated as a PCBF where the parameter corresponds to the look-backward time. Additionally, any CBF associated with a system exhibiting continuous symmetry, such as a mobile robot system invariant under translation in space, can also be regarded as a PCBF.

We validate the proposed control strategy through a simulation experiment using two examples. The simulation results well demonstrate that PCBF-QP successfully constrains the system's state within the prescribed region.

Notation

The set of reals and nonnegative reals are written as \mathbb{R} and $\mathbb{R}_{\geq 0}$, respectively. For positive integers l , m , and n , \mathbb{R}^l , $\mathbb{R}^{m \times n}$ denote the set of l -dimensional column vectors and matrices of size $m \times n$, respectively. By \mathbb{S}^n , we denote the set of symmetric square matrices of size $n \times n$, respectively. The inequalities between square matrices denote definiteness conditions: for example, for two symmetric square matrices $A, B \in \mathbb{S}^n$, $A \geq B$ means $A - B$ is positive semidefinite.

2. PRELIMINARIES

Consider the following nonlinear time-invariant control-affine system dynamics:

$$\dot{x} = f(x) + g(x)u, \quad (1)$$

where f and g are locally Lipschitz continuous functions, $x \in \mathbb{R}^n$ is state, $u \in \mathbb{R}^m$ is the control input. We assume that the control input is bounded by a set of linear inequalities:

$$u \in U = \{u \in \mathbb{R}^m : A_u u \leq b_u\} \quad (2)$$

where A_u and b_u are a matrix and a column vector with appropriate sizes.

For brevity, hereafter, we use the *dot* notation to denote the growth rate of a scalar function along the system's trajectory. Let $\zeta : \mathbb{R}^n \rightarrow \mathbb{R}$ be a differentiable function of state. The growth rate of ζ along the system's trajectory, $\dot{\zeta} : \mathbb{R}^n \times \mathbb{R}^m \rightarrow \mathbb{R}$ is defined as follows:

$$\dot{\zeta}(x, u) = \frac{\partial \zeta}{\partial x} \cdot (f(x) + g(x)u). \quad (3)$$

Similarly, if ζ also depends on time t , its time derivative along the trajectory becomes

$$\dot{\zeta}(x, u, t) = \frac{\partial \zeta}{\partial t} + \frac{\partial \zeta}{\partial x} \cdot (f(x) + g(x)u). \quad (4)$$

Control Barrier Functions

CBF is a powerful tool to guarantee set invariance of a controlled system. Its definition is as follows.

Definition 1 (Control Barrier Function (CBF)). A continuously differentiable function $h : \mathbb{R}^n \rightarrow \mathbb{R}$ is a CBF if there exists a class- \mathcal{K}_∞ function¹ $\alpha : \mathbb{R}_{\geq 0} \rightarrow \mathbb{R}$ such that

$$\max_{u \in U} \dot{h}(x, u) + \alpha(h(x)) \geq 0 \quad (5)$$

for all $x \in D_h = \{x \in \mathbb{R}^n : h(x) \geq 0\}$.

Definition 1 is equivalent to the existence of a feedback controller $u : \mathbb{R}^n \rightarrow U$ such that

$$\dot{h}(x, u(x)) + \alpha(h(x)) \geq 0 \quad (6)$$

for all $x \in D_h$. One easy way of synthesizing such controller is to formulate a QP, namely CBF-QP [5], to find one that minimally deviates from the reference input u_{ref} while satisfying the condition (6).

Problem 1 (CBF-QP).

$$\begin{aligned} u(x, u_{\text{ref}}) = \arg \min_{u \in U} \quad & \|u - u_{\text{ref}}\|^2 \\ \text{s.t.} \quad & \dot{h}(x, u) + \alpha(h(x)) \geq 0. \end{aligned} \quad (7)$$

The optimization problem (7) is surely a quadratic optimization problem if h is differentiable at x . It is well known that CBF-QP renders the set D_h invariant, and the optimization is always feasible given $x \in D_h$; i.e., CBF-QP is recursively feasible. Thanks to this property, if we can find a CBF h such that $h(x_f) < 0$ for any *forbidden* state x_f , CBF-QP will provide safety to the system given any reference input.

3. PARAMETRIZED CBF

We now introduce the notion of PCBF and formulate a QP-based control strategy using PCBF. Firstly, PCBF is defined as follows.

Definition 2 (Parametrized CBF (PCBF)). Let \mathcal{K} be the parameter space with a differentiable structure, i.e., a differentiable manifold. A continuously differentiable function $h : \mathbb{R}^n \times \mathcal{K} \rightarrow \mathbb{R}$ is a PCBF, if there exists a class- \mathcal{K}_∞ function α and a set of differentiable functions $\rho_i : \mathcal{K} \rightarrow \mathbb{R}$ ($i \in \mathcal{I}$), such that $h(x, k)$ is a CBF for all $k \in D_\rho = \{k : \rho_i(k) \geq 0, \forall i \in \mathcal{I}\}$.

We now formulate a CBF-QP-like control strategy that utilizes a PCBF. We use the notation $D_h(k)$ to denote the super zero level set of $h(\cdot, k)$, i.e.,

$$D_h(k) = \{x \in \mathbb{R}^n : h(x, k) \geq 0\}. \quad (8)$$

Note that, for every $k \in D_\rho$, $D_h(k)$ is invariant.

¹The function $\alpha : \mathbb{R}_{\geq 0} \rightarrow \mathbb{R}$ is a class- \mathcal{K}_∞ function if it is continuous, strictly increasing, unbounded, and $\alpha(0) = 0$.

Problem 2 (PCBF-QP).

$$\begin{aligned} (u, \dot{k}) = \arg \min_{u \in U, k \in T_k \mathcal{K}} \quad & \|u - u_{\text{ref}}\|^2 + \mu \|\dot{k}\|^2 \\ \text{s.t.} \quad & \dot{h}(x, k, u, \dot{k}) + \alpha(h(x, k)) \geq 0 \\ & \dot{\rho}_i(k, \dot{k}) + \alpha_{\rho}(\rho_i(k)) \geq 0 \quad \forall i \in \mathcal{I} \end{aligned} \quad (9)$$

Here, $\mu > 0$ is a tunable parameter employed to ensure numerical stability of the controller, $\alpha_\rho : \mathbb{R}_{\geq 0} \rightarrow \mathbb{R}$ is a class- \mathcal{K}_∞ function.

The optimization problem (9) is also a QP, given that h is differentiable at (x, k) and each ρ_i is differentiable at k . Practically, k serves as an internal state of the controller. The presence of \dot{k} allows the control strategy to select u from a broader feasible region, compared to that of the original CBF-QP. Through the following two propositions, we now verify that PCBF-QP also provides set invariance and recursive feasibility.

Proposition 1. If $x \in D_h(k)$ and $k \in D_\rho$, PCBF-QP is always feasible.

Proof. Since $k \in D_\rho$, $h(\cdot, k)$ with fixed k is a valid CBF. Therefore,

$$\max_{u \in U} \dot{h}(x, u, k, 0) + \alpha(h(x, k)) \geq 0. \quad (10)$$

Let u^* be the maximum argument of (10). Then, $(u^*, 0)$ is a feasible solution to PCBF-QP. In the last line of (9), with $\dot{k} = 0$, $\dot{\rho}_i = 0$ and since $\rho_i \geq 0$, $\alpha_\rho(\rho_i) \geq 0$. \square

Proposition 2. PCBF-QP renders the set $D_{h,\rho} = \{(x, k) : x \in D_h(k), k \in D_\rho\}$ invariant.

Proof. Observe that $\dot{h}(\dots) \geq 0$ if $h(\cdot) = 0$, and $\dot{\rho}_i(\dots) \geq 0$ if $\rho_i(\cdot) = 0$. It follows from Nagumo's theorem [12, 13] that $D_{h,\rho}$ is invariant. \square

As a corollary, the projection of the set $D_{h,\rho}$ onto the state space, i.e., $D_h = \bigcup_{k \in D_\rho} D_h(k)$ can be made invariant through PCBF-QP.

Finally, we point out that ρ_i can even be time-varying given that $\partial \rho_i / \partial t \geq 0$ everywhere, so that D_ρ , now as a set-valued function of time, always expands. The effect of positive $\partial \rho_i / \partial t \geq 0$ further broadens the feasible region of PCBF-QP.

4. EXAMPLES

4.1 Adaptive Cruise Control

As the first example, we consider the adaptive cruise control problem of a car on a one-dimensional road (see Fig. 1). The dynamics of the car is modeled as the following simple double integrator dynamics:

$$\dot{p} = v, \quad \dot{v} = u, \quad (11)$$

where $p \in \mathbb{R}$ and $v \in \mathbb{R}$ are the position and forward velocity of the car, respectively. The state variable is written as $x = [p, v]^\top \in \mathbb{R}^2$, and $u \in \mathbb{R}$ is the acceleration input.

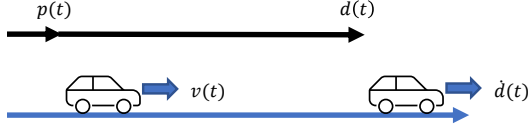


Fig. 1. The adaptive cruise control example. The left car is the ego vehicle, whose goal is to not collide with the vehicle in the front. The ego vehicle's maximum acceleration and deceleration are bounded. We neglect the size of the vehicle.

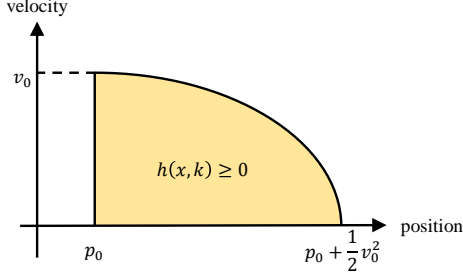


Fig. 2. The PCBF (12) designed for the adaptive cruise control example. The yellow region denotes where the $h(x, k)$ value is nonnegative. This PCBF takes in a two-dimensional parameter $k = [p_0, v_0]^\top$, where $p_0 \in \mathbb{R}$ and $v_0 \in \mathbb{R}$.

For the sake of simplicity of formulation, we ignore the size of the car.

The goal of the ego vehicle is to move forward as fast as possible, while complying with the following rules:

1. The input acceleration should not exceed the limit $u \in U = [-1, 1] \subset \mathbb{R}$.
2. The vehicle should always move forward, and its speed should not exceed the maximum speed limit $v_{\max} = 4$; i.e., $0 \leq v \leq 4$.
3. It should not collide with the vehicle in the front. The position of the front vehicle is written as d . We assume that the front vehicle always moves forward, i.e., $\dot{d}(t)$, as a function of time, is always increasing. Thus, the constraint is written as $p \leq d$.

A PCBF for this system is designed as follows:

$$h(x, k) = \min \left\{ (p_0 - p) + \frac{1}{2}(v_0^2 - v^2), v, p - p_0 \right\}, \quad (12)$$

where $k = [p_0, v_0]^\top \in \mathbb{R}^2$ is the parameter. A brief graphical description of the set $D_h(k)$ is drawn in Fig. 2. In the following proposition, we verify that (12) is a valid PCBF for the system (11) with bounded input $u \in U$.

Proposition 3. *Eq. (12) is a valid PCBF for the system given $v_0 \geq 0$, for any class- \mathcal{K}_∞ function α such that $\alpha(y) \geq y$ for all $y \geq 0$.*

Proof. See the appendix. \square

To make $h(x, k)$ safe, we set up the following con-

straints on the parameter k .

$$\begin{aligned} \rho_1(k, t) &= d(t) - \left(p_0 + \frac{1}{2}v_0^2 \right) \geq 0 \\ \rho_2(k) &= v_0 \geq 0 \\ \rho_3(k) &= v_{\max} - v_0 = 4 - v_0 \geq 0 \end{aligned} \quad (13)$$

Here, ρ_1 is also a function of time: the assumption that $\dot{d}(t) \geq 0$ guarantees that $\partial \rho_1 / \partial t \geq 0$. Finally, we let $u_{\text{ref}} = 1$ in order to make the vehicle proceed as fast as possible.

Therefore, we setup the PCBF-QP as follows.

$$\begin{aligned} (u, \dot{k}) &= \arg \min_{u, \dot{k}} (u - 1)^2 + \mu(\dot{p}_0^2 + \dot{v}_0^2) \\ \text{s.t. } &\dot{h}(x, k, u, \dot{k}) + \gamma_h h(x, k) \geq 0 \\ &\dot{d}(t) - \dot{p}_0 - v_0 \dot{v}_0 \\ &\quad + \gamma_\rho \cdot \left(d(t) - \left(p_0 + \frac{1}{2}v_0^2 \right) \right) \geq 0 \\ &\dot{v}_0 + \gamma_\rho v_0 \geq 0 \\ &-\dot{v}_0 + \gamma_\rho(4 - v_0) \geq 0 \end{aligned} \quad (14)$$

Here, we let $\mu = 0.1$, $\alpha(y) = \gamma_h y$, and $\alpha_\rho(y) = \gamma_\rho y$, where $\gamma_h = 5$, and $\gamma_\rho = 1$.

Using MATLAB's `ode45` ordinary differential equation solver and `quadprog` QP solver, we present the simulation result within the duration $t \in [0, 15]$ in three different scenarios. In all three scenarios, the initial condition is given as $x(0) = [0, 0]^\top$ and $k(0) = [-0.25, 1]^\top$.

4.1.1 $d(t) = 20$

In the first scenario, the front vehicle is at a complete stop at $d = 20$. The goal of the ego vehicle, therefore, is to first move forward and decelerate to a stop at $p = 20$. The results (Fig. 3 (a)) clearly show that the safety constraints are satisfied throughout the mission, i.e., the PCBF and the ρ values are kept nonnegative at all times.

4.1.2 $d(t) = 2 + 2t$

In the second scenario, the front vehicle moves at constant speed of $\dot{d}(t) = 2$, starting from the initial position $d(0) = 2$. It can be seen from the result (Fig. 3 (b)), that the ego vehicle follows the leading vehicle while maintaining a safe distance.

4.1.3 $d(t) = \min\{2 + t, 10\}$

In the third scenario, the leader first proceeds at a constant speed of $\dot{d} = 1$ and then suddenly stops at time $t = 8$. Even in this case, as shown in Fig. 3 (c), the ego vehicle was able to come to a complete stop right before the leading vehicle.

4.2 Constraining a Linear System

As the second example, we consider the problem of constraining a linear system near the origin. We use the following model with two-dimensional state space and one-dimensional input:

$$\dot{x} = Ax + Bu = \begin{bmatrix} 0 & 1 \\ 0 & 0 \end{bmatrix} x + \begin{bmatrix} 0 \\ 1 \end{bmatrix} u, \quad (15)$$

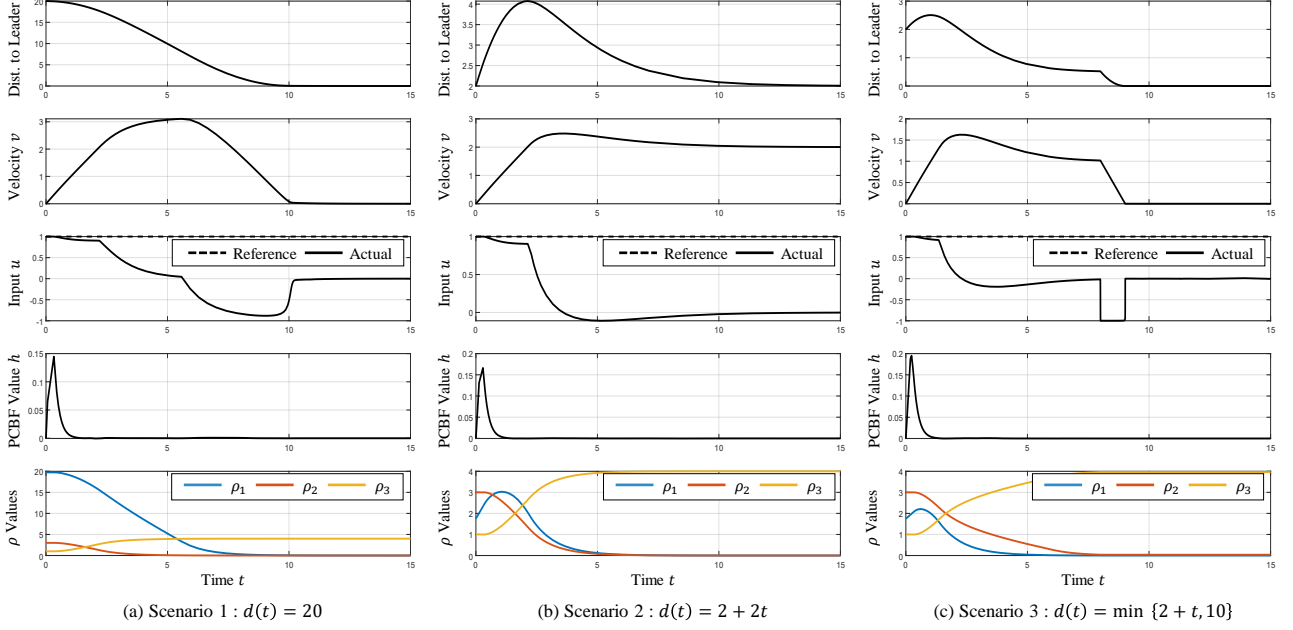


Fig. 3. Simulation result. (a) The ego vehicle first accelerates to obtain enough speed, and then gradually decelerates to stop at $p = 20$. (b) The ego vehicle maintains a safe distance to the vehicle in the front. Its speed therefore converges to the front vehicle's speed, 2. (c) Right after the sudden stop, the ego vehicle decelerates to its capacity in order to safely stop right before the leading vehicle.

where the input is constrained by the inequality $-1 \leq u \leq 1$, and the goal is to keep the state variable within the region

$$-1 \leq y = \begin{bmatrix} 1 & 0 \end{bmatrix} x \leq 1 \quad (16)$$

while exerting input u that minimally deviates from the reference input $u_{\text{ref}}(t) = 0.5 + \cos(6t)$. For that, we design the following PCBF:

$$h(x, k) = b - \frac{1}{2}x^\top Px, \quad (17)$$

where $k = (b, P, K)$, $b \in \mathbb{R}$, $P \in \mathbb{S}^2$, $K \in \mathbb{R}^{1 \times 2}$. Although the PCBF does not explicitly depend on the third parameter K , it is used as a slack variable when formulating the safety constraints.

The safety constraints are as follows.

1. To make $h(\cdot, k)$ a CBF, we first require

$$V = \frac{1}{2}x^\top Px \quad (18)$$

to be a control Lyapunov function for the system without the input constraints. There must exist a feedback gain K such that

$$\begin{aligned} \dot{V}(x, -Kx) \\ = \frac{1}{2}x^\top (P(A - BK) + (A - BK)^\top P)x \leq 0 \end{aligned} \quad (19)$$

for all x , therefore we let

$$\rho_1(k) = -P(A - BK) - (A - BK)^\top P \geq 0. \quad (20)$$

2. The feedback input $u = -Kx$ should satisfy the input constraints for all $x \in D_h(k) = \{x : \frac{1}{2}x^\top Px \leq b\}$. We rewrite this condition as

$$D_h(k) \subseteq \{x : \|Kx\|^2 \leq 1\}, \quad (21)$$

which is equivalent to

$$\rho_2(k) = P - 2bK^\top K \geq 0. \quad (22)$$

3. The state should satisfy the constraint (16), which can be rewritten as

$$D_h(k) \subseteq \left\{x : x^\top \begin{bmatrix} 1 & 0 \\ 0 & 0 \end{bmatrix} x \leq 1\right\}. \quad (23)$$

This is equivalent to

$$\rho_3(k) = P - \begin{bmatrix} 2b & 0 \\ 0 & 0 \end{bmatrix} \geq 0. \quad (24)$$

Note that the parameter constraints (20), (22), and (24) are expressed in linear matrix inequality (LMI) form, rather than scalar inequalities. To deal with this, we first let $\alpha_\rho(y) = \gamma_\rho y$ and replace the inequality constraint with the LMI constraint $\dot{\rho} + \gamma_\rho \cdot \rho \geq 0$. A good interpretation to this is that we translated an infinite number of inequality constraints into one single LMI form, i.e., if $A \in \mathbb{S}^r$,

$$\begin{aligned} \frac{d}{dt} (\xi^\top A \xi) + \gamma \cdot (\xi^\top A \xi) &\geq 0, \quad \forall \xi \in \mathbb{R}^r \\ \iff \dot{A} + \gamma \cdot A &\geq 0. \end{aligned} \quad (25)$$

The simulation was conducted within the interval $t \in [0, 2.5]$ with initial condition $x(0) = 0$. The parameters P and K were initialized using the linear quadratic regulator (LQR) technique and $b(0)$ was set to a very small positive number (10^{-6}). The simulation used MATLAB's ode45 ordinary differential equation solver and CVX [14] with SDPT3 [15] convex optimization solver. The results are shown in Fig. 4 and Fig. 5: it can be seen from

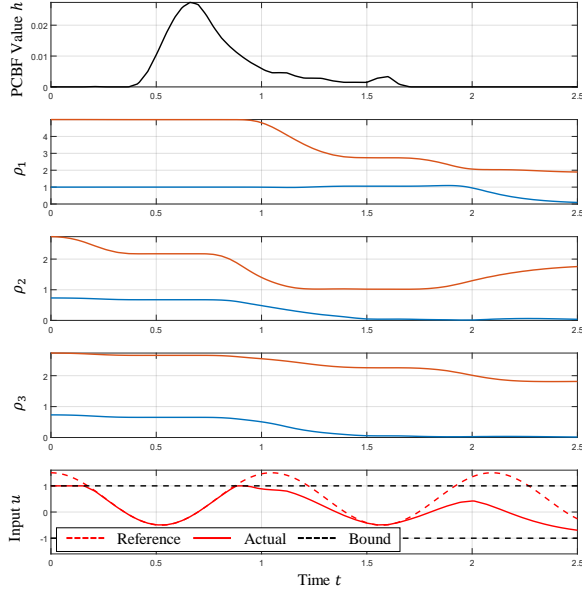


Fig. 4. Simulation results for the second example. To check the positive definiteness of the LMI constraints $\rho(\cdot)$, the two eigenvalues of $\rho(\cdot)$ are plotted here. The PCBF and ρ values are kept positive (semidefinite) throughout the interval. It can also be seen that the input constraints are satisfied, although the reference input u_{ref} exceeds the limit sometimes.

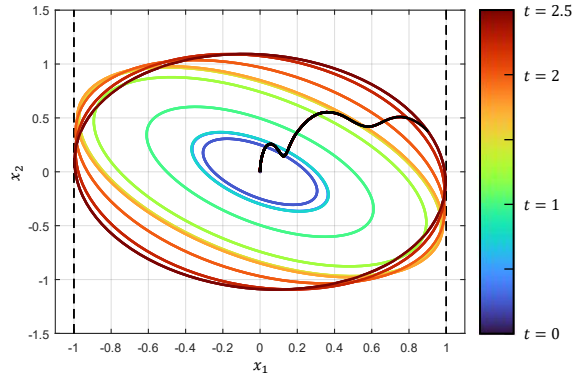


Fig. 5. The phase portrait of the system's trajectory, drawn along with the trace of $D_h(k)$. The black curve represents the trajectory, dashed lines represent the constraint (16). The colored ellipses denote the boundaries of $D_h(k)$, where the colors represent the flow of time. The system and the set $D_h(k)$ are well contained within the bound throughout the simulation.

the plots that the LMI safety constraints are met throughout the simulation, and the PCBF value is always kept nonnegative. It is notable that not only the size of the ellipse but also its shape changes: PCBF-QP automatically deformed the ellipse, so that the generated input better tracks the reference without violating the safety constraints.

5. CONCLUSION

In this paper, we introduced PCBF, a parametrized continuous spectrum of CBFs for a controlled system. We also formulate a CBF-QP-like control strategy using PCBF, namely PCBF-QP. PCBF-QP searches for the best choice of input that is closest to the given reference,

under the set invariance constraints. We provide a brief proof that the proposed PCBF-QP renders the super zero level set of PCBF invariant, and it is recursively feasible. The proposed control strategy was validated in simulation experiments using two different settings. Through the result, we observe that PCBF-QP serves as a valid safety-critical controller for the system.

For future work, we will investigate ways to systematically synthesize PCBFs given the model and safety constraints using, for example, neural networks [16], Hamilton-Jacobi reachability analysis [17], etc. Also, we will develop a *robust* version of PCBF, so that PCBF-QP becomes capable of dealing with model uncertainties and unmodeled exogenous disturbing forces.

ACKNOWLEDGMENT

This research was supported by Unmanned Vehicles Core Technology Research and Development Program through the National Research Foundation of Korea (NRF) and Unmanned Vehicle Advanced Research Center(UVARC) funded by the Ministry of Science and ICT, the Republic of Korea (NRF2020M3C1C1A010864).

REFERENCES

- [1] S. Kousik, S. Vaskov, F. Bu, M. Johnson-Roberson, and R. Vasudevan, "Bridging the gap between safety and real-time performance in receding-horizon trajectory design for mobile robots," *The International Journal of Robotics Research*, vol. 39, no. 12, pp. 1419–1469, 2020.
- [2] M. Chen, S. L. Herbert, H. Hu, Y. Pu, J. F. Fisac, S. Bansal, S. Han, and C. J. Tomlin, "Fastrack: a modular framework for real-time motion planning and guaranteed safe tracking," *IEEE Transactions on Automatic Control*, vol. 66, no. 12, pp. 5861–5876, 2021.
- [3] X. Xu, J. W. Grizzle, P. Tabuada, and A. D. Ames, "Correctness guarantees for the composition of lane keeping and adaptive cruise control," *IEEE Transactions on Automatic Science and Engineering*, vol. 15, no. 3, pp. 1216–1229, 2017.
- [4] A. D. Ames, S. Coogan, M. Egerstedt, G. Notomista, K. Sreenath, and P. Tabuada, "Control barrier functions: Theory and applications," in *2019 18th European Control Conference (ECC)*, 2019, pp. 3420–3431.
- [5] A. D. Ames, X. Xu, J. W. Grizzle, and P. Tabuada, "Control barrier function based quadratic programs for safety critical systems," *IEEE Transactions on Automatic Control*, vol. 62, no. 8, pp. 3861–3876, 2017.
- [6] M. Jankovic, "Robust control barrier functions for constrained stabilization of nonlinear systems," *Automatica*, vol. 96, pp. 359–367, 2018.
- [7] W. Xiao, C. Belta, and C. G. Cassandras, "Adap-

- tive control barrier functions,” *IEEE Transactions on Automatic Control*, vol. 67, no. 5, pp. 2267–2281, 2021.
- [8] Q. Nguyen and K. Sreenath, “Exponential control barrier functions for enforcing high relative-degree safety-critical constraints,” in *2016 American Control Conference (ACC)*. IEEE, 2016, pp. 322–328.
- [9] W. Xiao and C. Belta, “Control barrier functions for systems with high relative degree,” in *2019 IEEE 58th conference on decision and control (CDC)*. IEEE, 2019, pp. 474–479.
- [10] L. Wang, A. D. Ames, and M. Egerstedt, “Safety barrier certificates for collisions-free multirobot systems,” *IEEE Transactions on Robotics*, vol. 33, no. 3, pp. 661–674, 2017.
- [11] S. Bansal, M. Chen, S. Herbert, and C. J. Tomlin, “Hamilton-jacobi reachability: A brief overview and recent advances,” in *2017 IEEE 56th Annual Conference on Decision and Control (CDC)*. IEEE, 2017, pp. 2242–2253.
- [12] F. Blanchini and S. Miani, *Set-theoretic methods in control*. Springer, 2008, vol. 78.
- [13] F. Blanchini, “Set invariance in control,” *Automatica*, vol. 35, no. 11, pp. 1747–1767, 1999.
- [14] M. Grant and S. Boyd, “CVX: Matlab software for disciplined convex programming, version 2.1,” <http://cvxr.com/cvx>, Mar. 2014.
- [15] K.-C. Toh, M. J. Todd, and R. H. Tütüncü, “Sdpt3—a matlab software package for semidefinite programming, version 1.3,” *Optimization methods and software*, vol. 11, no. 1-4, pp. 545–581, 1999.
- [16] W. Xiao, T.-H. Wang, R. Hasani, M. Chahine, A. Amini, X. Li, and D. Rus, “Barriernet: Differentiable control barrier functions for learning of safe robot control,” *IEEE Transactions on Robotics*, 2023.
- [17] J. J. Choi, D. Lee, K. Sreenath, C. J. Tomlin, and S. L. Herbert, “Robust control barrier-value functions for safety-critical control,” in *2021 60th IEEE Conference on Decision and Control (CDC)*. IEEE, 2021, pp. 6814–6821.

APPENDIX: PROOF OF PROPOSITION 3

Proof. To verify (12) is a PCBF, we assume that k is kept constant with respect to time and view it as an ordinary CBF. For brevity, we use the shorthand notation $h_0(x) = (p_0 - p) + \frac{1}{2}(v_0^2 - v^2)$, $h_1(x) = v$, and $h_2(x) = p - p_0$.

We will show the closed-loop system under the feedback law

$$u(x) = \begin{cases} -1 & h_0(x) < h_1(x) \\ -v/(1+v) & h_0(x) = h_1(x) \\ 1 & h_0(x) > h_1(x) \end{cases} \quad (26)$$

satisfies

$$\dot{h}(x, k, u, 0) + h(x, k) \geq 0, \quad (27)$$

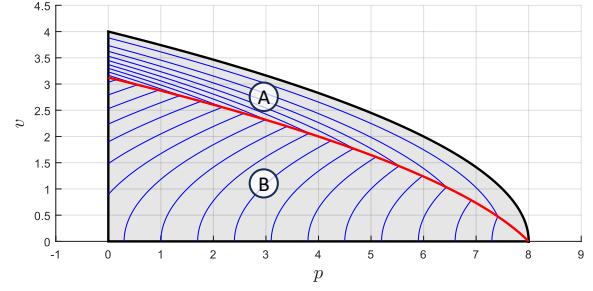


Fig. 6. The closed-loop trajectories (blue curves) under the feedback law (26). In regions \textcircled{A} and \textcircled{B} (not including the red curve), the CBF value along the trajectory is a nondecreasing function. Along the red curve, the CBF value decreases not faster than the exponential decay rate e^{-t} . In this figure, $p_0 = 0$, $v_0 = 4$.

for any fixed k such that $v_0 \geq 0$. Note that since $v \geq 0$ everywhere on $D_h(k)$, $u(x) \in [-1, 1]$.

For that, we first show that the closed-loop system reaches the surface $h_0(x) = h_1(x)$ (the red curve in Fig. 6) in finite time, and (26) keeps the system on the surface afterwards. Let $V(x) = |h_0(x) - h_1(x)|$. If $h_0(x) < h_1(x)$ (region \textcircled{A} in Fig. 6),

$$\dot{V}(x, u(x)) = \dot{h}_1(x, -1) - \dot{h}_0(x, -1) = -1. \quad (28)$$

And if $h_0(x) > h_1(x)$ (region \textcircled{B} in Fig. 6),

$$\dot{V}(x, u(x)) = \dot{h}_0(x, 1) - \dot{h}_1(x, 1) = -1 - 2v \leq -1. \quad (29)$$

In both cases, the decrement of V is bounded strongly away from zero, and thus it reaches the surface $h_0(x) = h_1(x)$ in finite time. After reaching the surface, the state is constrained on it, since

$$\begin{aligned} \dot{h}_0(x, u(x)) - \dot{h}_1(x, u(x)) &= -v - vu(x) - u(x) \\ &= -v + \frac{v^2}{1+v} + \frac{v}{1+v} = 0. \end{aligned} \quad (30)$$

The closed-loop trajectory is therefore well-defined.

Next, we show that $h(x, k)$ along the closed-loop trajectory satisfies (27). Firstly, since $v \geq 0$ everywhere on the domain $D_h(k)$, $h_2 = p - p_0$ never decreases. If $h_0(x) < h_1(x)$ (region \textcircled{A} in Fig. 6),

$$\dot{h}_0(x, u(x)) + h_0(x) = -v + vu(x) + h_0(x) = h_0(x) \geq 0. \quad (31)$$

If $h_0(x) = h_1(x)$ (red curve in Fig. 6), $h_0(x) = h_1(x) = v$ along the trajectory, thus

$$\begin{aligned} \dot{h}_0(x, u(x)) + h_0(x) &= \dot{h}_1(x, u(x)) + h_1(x) \\ &= u(x) + v = \frac{v^2}{1+v} \geq 0, \end{aligned} \quad (32)$$

i.e., the inequality holds for both h_0 and h_1 . And finally, if $h_0(x) > h_1(x)$ (region \textcircled{B} in Fig. 6),

$$\dot{h}_1(x, u(x)) + h_1(x) = v + u(x) = v + 1 \geq 0. \quad (33)$$

Therefore, we conclude that the CBF value satisfies (6) everywhere on $D_h(k)$. \square